Absorption enhancement and sensing properties of Ag diamond nanoantenna arrays*

Yuan Yu-Yang(袁宇阳)[a], Yuan Zong-Heng(袁纵横)[a)b)†], Li Xiao-Nan(李骁男)[a], Wu Jun(吴 军)[a], Zhang Wen-Tao(张文涛)[a], and Ye Song(叶 松)[a]

[a] School of Electronic Engineering and Automation, Guilin University of Electronic Technology, Guilin 541004, China
[b] School of Information Engineering, Guizhou Minzu University, Guiyang 550025, China

(Received 19 August 2014; revised manuscript received 14 January 2015; published online 29 May 2015)

Noble metal nanoantenna could effectively enhance light absorption and increase detection sensitivity. In this paper, we propose a periodic Ag diamond nanoantenna array to increase the absorption of thin-film solar cells and to improve the detection sensitivity via localized surface plasmon resonance. The effect of nanoantenna arrays on the absorption enhancement is theoretically investigated using the finite difference time domain (FDTD) method with manipulating the spectral response by geometrical parameters of nanoantennas. A maximum absorption enhancement factor of 1.51 has been achieved in this study. In addition, the relation between resonant wavelength (intensity reflectivity) and refractive index is discussed in detail. When detecting the environmental index using resonant wavelengths, a maximum detection sensitivity of about 837 nm/RIU (refractive index unit) and a resolution of about 10^{-3} RIU can be achieved. Moreover, when using the reflectivity, the sensitivity can be as high as 0.93 AU/RIU. Furthermore, we also have theoretically studied the effectiveness of nanoantennas in distinguishing chemical reagents, solution concentrations, and solution allocation ratios by detecting refractive index. From the results presented in this paper, we conclude that this work might be useful for biosensor detection and other types of detections.

Keywords: surface plasmon resonance, nanoantenna, finite difference time domain (FDTD), sensor

PACS: 42.50.Wk **DOI:** 10.1088/1674-1056/24/7/074206

1. Introduction

Metal nanoantenna is a type of nanometer structure device, which generally consists of metal nanoparticles and can effectively couple the energy from free space to sub-wavelength scales. Noble metal nanoantennas made from gold, silver, and copper could induce localized surface plasmon resonance (LSPR) and such effect has been extensively studied. This unique feature determines their wide applications in molecular sensing,[1,2] metamaterials,[3] enhanced nonlinearities,[4] terahertz application,[5] thin-film solar cells,[6] and etc.

Thin-film solar cells have attracted great attention due to their potential to reduce photovoltaic device cost. However, semiconductor substrates such as silicon and GaAs suffer from weak absorption at red and near-infrared wavelengths.[7,8] To enhance optical absorption of solar cells, metal nanoantennas can be deposited on the surfaces. As have been demonstrated, metal nanoantennas, which could induce LSPR, significantly improve light absorption in solar cells.[9,10] With strong light scattering properties, they could increase the optical path length within solar cells, thus reducing requirement of active layer thickness. In addition, noble metal nanoantennas have been widely used in LSPR-based sensors.[11,12] It is well known that the LSPR properties of noble metal nanoantennas are dependent on their sizes, shapes, and the dielectric constant of the surrounding medium.[13] Meanwhile, the LSPR is also sensitive to the refractive index change in the vicinity of the metal surface, while the resonant wavelength and angle are closely related to the characteristics of the test substance near the metal surface. The resonant wavelength and angle of the LSPR will change according to the changes of the refractive index of the medium. This allows the refractive index change to be detected via resonant wavelength and angle detection, which is the principle used when designing SPR sensors.[14,15] Up to now, noble metal nanoantennas have been successfully used in biosensors, optical fiber sensors, and so on. For both thin-film solar cells and SPR sensors, many nanostructures, such as dipole antenna,[16,17] bow-tie antenna,[18] and nano-disk antenna,[19] are designed for relatively effective absorption and sensing. However, in order to develop more efficient thin-film solar cells and more sensitive SPR sensors, it is worth searching and investigating new nanoantennas. In this study, we aim to develop new nanoantennas which can be used in thin-film solar cells and SPR sensors.

In this paper, we present a newly designed nanoantenna and carry out detailed investigations via numerical finite difference time domain (FDTD) solutions. This type of nanoantenna consists of periodic array of diamond nanoparticles. The

*Project supported by the International Scientific and Technological Cooperation Projects of Guizhou Province, China (Grant No. 20117035) and the Program for Innovative Research Team of Guilin University of Electronic Technology, China (Grant No. IRTGUET).

†Corresponding author. E-mail: yuanzongheng@sina.com

© 2015 Chinese Physical Society and IOP Publishing Ltd

effect of nanoantennas on optical absorption enhancement in thin-film silicon solar cells is discussed with detailed analyses and interpretations. Some investigations have been carried out upon the application of diamond nanoantennas in detecting environmental indices as well as the relation between detection parameters and refractive indices. Moreover, the effectiveness of diamond nanoantennas in detecting refractive indices, especially for types of chemical reagents, solution concentration determination, and different allocation ratios of solution, is also studied.

2. Model and simulation method

The nanoantenna array designed using diamond nanoparticles is illustrated in Fig. 1. The diamond nanoantennas consisting of Ag nanoparticles are uniformly distributed on a 500-nm-thick silicon substrate. The geometrical parameters of the nanostructure are the height (h) and the period of the nanoparticle array in the x direction (P_x) and y direction (Py). The top view of a diamond nanoparticle is depicted in Fig. 1(b), the solid line represents the short axis length (a) of the diamond, while the dotted line represents the long axis length (b) of the diamond. We choose Ag nanoparticles here because of its obvious LSP effects. The optical parameters of silicon and Ag are all taken from Ref. [20].

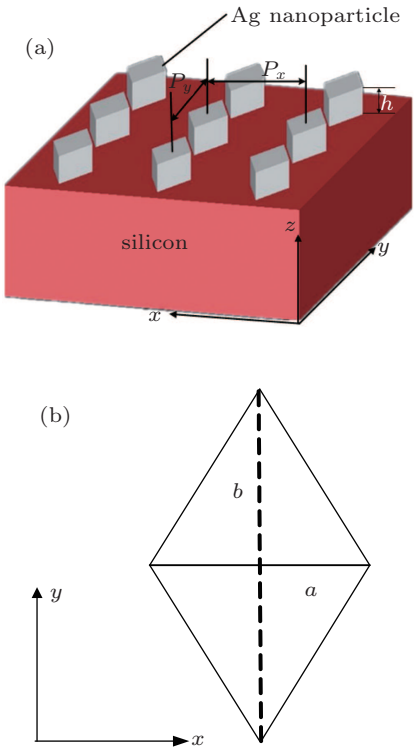


Fig. 1. (color online) (a) Geometry of the diamond nanoantenna arrays. (b) Top view of a diamond nanoparticle.

Numerical analyses are carried out using FDTD simulations. The illumination source perpendicular to the structure is polarized to the x direction with its wavelength ranging from 400 to 1100 nm. Perfectly matched layers (PML) are used in the incident direction to prevent any interference effect. Periodic boundary conditions are used at the lateral (x–y) boundaries of the simulation volume. The metal nanoantennas are generally treated as light trapping structures, we define the absorption of solar cells as the absorption in the silicon layer, and the bare solar cell as the solar cell without any light trapping structures. For simplicity, we assume each photon with energy greater than the band gap can be absorbed to produce one electron–hole pair. Here, we use the absorption enhancement G to quantify the improvement of light absorption when metal nanoantennas are applied. The G is given by

$$G = \frac{\mathrm{IQE_{particle}}}{\mathrm{IQE_{bare}}} = \frac{\int \lambda P_{\mathrm{t}}(\lambda) I_{\mathrm{AM1.5}}(\lambda)\,\mathrm{d}\lambda}{\int \lambda P_{\mathrm{bare}}(\lambda) I_{\mathrm{AM1.5}}(\lambda)\,\mathrm{d}\lambda}, \tag{1}$$

where $I_{\mathrm{AM1.5}}$ is the AM 1.5 solar spectrum,[21] and IQE is the integrated quantum efficiency of a solar cell, with subscript "particle" and "bare" denoting solar cells with nanoparticles and bare silicon solar cells. $P_{\mathrm{t}}(\lambda)$ and $P_{\mathrm{bare}}(\lambda)$ stand for the light absorption of silicon layer with and without metal nanoantennas, respectively.

For SPR sensors, metal nanoantenna arrays are treated as detection structures. Here, metal nanoantennas and silicon substrate form a simple sensing device. The sensitivity of SPR sensor, S, can be calculated by

$$S = \frac{\Delta t}{\Delta n}, \tag{2}$$

where Δn represents the refractive index change of the test substance, and Δt represents the corresponding change of the detection parameters (resonant wavelength, resonant angle, etc.).

3. Results and discussion

Figure 2 illustrates the change of absorption with h and P_y, respectively. Figure 2(a) shows the absorption of silicon with h and fixed a, b, and p. As we can see, compared with that of bare solar cells, light absorption is greatly enhanced when nanoantennas are applied. The value of G achieves 1.28, 1.36, 1.33 and 1.27 for $h = 40$, 60, 80 and 100 nm, respectively. The value of G increases with h when it is below 60 nm, but decreases afterwards. This can be understood that when the height h increase, the phase shift between the scattering field and the incident field change periodically, and weaken the electromagnetic field, then reduce absorption. Besides, Ag nanoparticles absorb more light as the height increases, both of reasons result in this phenomenon. Particularly, in the near-infrared region, the absorption enhancement effect is strong due to the LSPR effects induced by Ag nanoantennas. From Fig. 2(b), we set $P_x = 100$ nm, $a = b = 65$ nm, and $h = 60$ nm. When P_y increases from 80 to 140 nm with a 20-nm step, the value of G equals 1.29, 1.37, 1.34, and 1.3, respectively, which indicates the absorption is also significantly enhanced. For

both cases, the absorption enhancement results from the scattering effect of Ag nanoantennas induced LSPR effect. The results also suggest that h and p have significant impacts on the LSPR effect of nanoantennas and thus the absorption enhancement of solar cells.

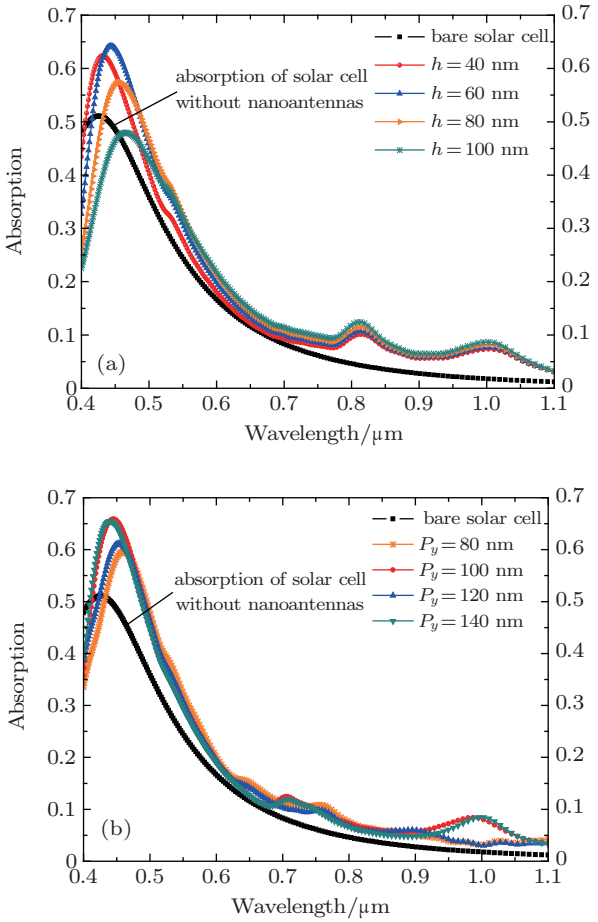


Fig. 2. (color online) (a) Absorption spectra of solar cell. $P_x = P_y =$ 100 nm, $a = b = 65$ nm, h is 40, 60, 80, 100 nm, respectively. (b) Absorption spectra of solar cell. $P_x = 100$ nm, $a = b = 65$ nm, $h = 60$ nm, P_y is 80, 100, 120, 140 nm, respectively.

Figures 3(a) and 3(b) show the change of absorption with a and b, respectively. As shown in Fig. 3(a), compared with that of bare solar cells, the absorption is enhanced in the entire wavelength range when nanoantennas are applied. For $b = 20$, 40, 60, and 80 nm, the value of G achieves 1.15, 1.25, 1.28, and 1.3, respectively. With fixed short axis length, the change of the long axis length causes the change of distance between diamond nanoparticles, thus changing the LSPR effect and the absorption enhancement. In the visible range, although the absorption peak does not change significantly when b increases, the peak value increases remarkably. The largest peak value, 0.66, appears at a wavelength of 426 nm and $b = 80$ nm. In the near-infrared region, the absorption enhancement is even stronger. With the increase of b, we could observe more resonance peaks due to the LSPR effects. Due to coupling between the Fabry–Perot resonance inside the nanoantenna and LSPR, with the increase of b, the resonance mode increases, causing more resonance peaks. Figure 3(b) shows that when $a = 10$, 20, 30, and 40 nm, the value of G achieves 1.11, 1.3, 1.27, and 0.66, respectively. Strangely, when $a = 40$ nm, the absorption of solar cells with diamond nanoantennas is below that of bare solar cells, which can be explained as follows. When $a = 40$ nm, a is equal to P_x, which means that Ag nanoparticles are close to each other, weakening the LSPR effect. Meanwhile, the surface dimension of diamond increases significantly, thus the reflection and absorption of Ag itself also reduce the absorption in silicon. From Fig. 3, we could conclude that the choice of a and b could strongly affect the absorption enhancement in solar cells.

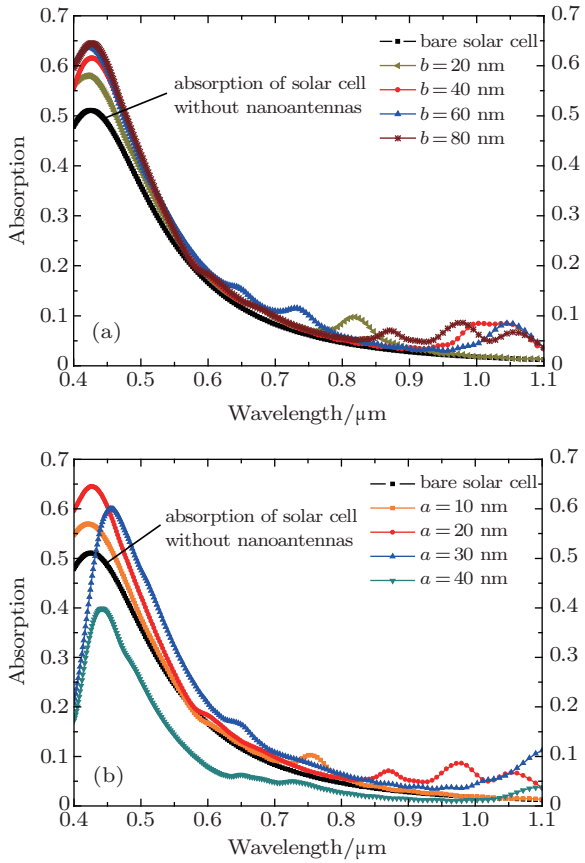


Fig. 3. (color online) (a) Absorption spectra of solar cell. $P_x = 40$ nm, $P_y = 90$ nm, $h = 60$ nm, $a = 20$ nm, b is 20, 40, 60, 80 nm, respectively. (b) Absorption spectra of solar cell. $P_x = 40$ nm, $P_y = 90$ nm, $h = 60$ nm, $b = 80$ nm, a is 10, 20, 30, 40 nm, respectively.

Comprehensive optimization yields that the optimal parameters of diamond nanoantennas are $h = 60$ nm, $P_x = 30$ nm, $P_y = 90$ nm, $a = 20$ nm, and $b = 85$ nm with a maximum G value of 1.51. To conclude, due to the LSPR effect, metal nanoantennas could significantly increase the absorption of thin-film solar cells by 50% to a largest extent. Ag diamond nanoantennas not only effectively enhance light absorption, but can also be applied in detection. Diamond nanoantennas show a strong plasmonic effect at the boundary with a dielectric material. Given this unique property, we also present its application in the detection of environmental refraction indices

and solution concentrations in this section. We firstly investigate the influence of environmental indices on the resonance spectrum by maintaining the simulation conditions and vertical light incident angle. The results are summarized in Fig. 4.

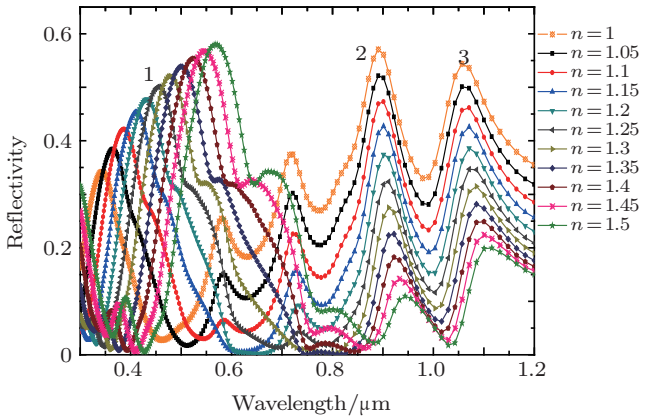


Fig. 4. (color online) Resonant spectrum as a function of index with an increment of 0.05 RIU.

As can be seen from Fig. 4, due to the multi-resonance characteristics of diamond nanoantennas, we choose three obvious resonance areas as the detection areas. In area 1, it exhibits a clear trend of the alteration of the resonance spectrum where the index increases from 1 to 1.5 with a step of 0.05. The resonance wavelength shifts about 203 nm, while the reflectivity peak value increases slowly as the index increases. In areas 2 and 3, the resonance wavelength moves with increasing index slightly, while the reflectivity peak experiences obvious changes. These results suggest that in area 1, the resonance wavelength is more suitable for monitoring the refractive index change. While in areas 2 and 3, the reflectivity at a fixed wavelength is more suitable for detecting the refractive index change. As a result, we treat resonance wavelength and reflectivity as two detection parameters. As diamond nanoantennas could provide a variety of detection methods, the flexibility of detection can be improved. Data presented in Fig. 4 are reproduced in Fig. 5, showing the relationship between reflectivity (resonance wavelength) and index.

As shown in Fig. 5, with increasing index, both the resonant wavelength and reflection peak undergo almost linear changes. From Figs. 5(a) and 5(b), in area 1, the sensitivity of reflectivity is 0.456 AU/RIU as calculated by Eq. (2). Besides, the resonant wavelength moves towards longer wavelengths with a slope of about 46 nm/0.1 RIU. From Figs. 5(c) and 5(d), in areas 2 and 3, the sensitivity of reflectivity is 0.924 and 0.688 AU/RIU, respectively, and the sensitivity of resonant wavelength is 106 and 86 nm/RIU, respectively. The results are in good agreement with Fig. 4. Moreover, the conclusion demonstrates the feasibility of diamond nanoantennas in refractive index detection.

To further improve the detection sensitivity, factors that influence the sensitivity are analyzed below. Here, we present detailed discussion on the effect of incident angle. Meanwhile, to simplify the comparison, the detection sensitivity of the resonant wavelength in area 1 is also discussed here. Figure 6(a) shows the reflection spectrum when the incident angle is 30°. We can see that the resonance amplitude in area 1 decreases more sharply compared with that in Fig. 4, while the resonance wavelength still experiences obvious changes. In area 2, the resonance amplitude also decreases, but in area 3, the resonance amplitude increases drastically and the bandwidth of the resonance spectrum becomes wider.

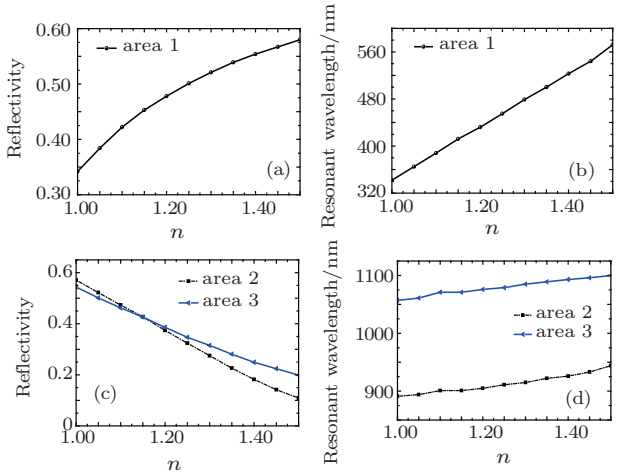


Fig. 5. (color online) Resonant wavelength and reflection peak value as functions of index n with an increment step of 0.05 (a) reflectivity in area 1, (b) resonance wavelength in area 1, (c) reflectivity in areas 2 and 3, and (d) resonance wavelength in areas 2 and 3.

Figure 6(b) shows the relationship between resonant wavelength and index with different incident angles. For all the three angles studied, the resonant wavelength almost increases linearly with the index. The sensitivities of the resonant wavelength are 771, 707, and 664 nm/RIU for incident angles of 30°, 45°, and 60°, respectively. Therefore, we can see that the incident angle of light source has a significant impact on the sensitivity.

As a result, to obtain even higher detection sensitivity, we use the same analytical method to further optimize the incident angle. With an ideal incident angle of 15°, the maximum sensitivity of the resonant wavelength in area 1 reaches 837 nm/RIU. When we measure the change of refractive index by detecting the change of resonance wavelength with the USB4000-VIS-NIR spectrometer which can detect a wavelength change of 0.3 nm, then we obtain a resolution approaching 10^{-3} RIU. Similarly, in area 3, the maximum sensitivity of intensity reflectivity reaches 0.93 AU/RIU. Compared with other sensitivity results reported in the literature (as listed in Table 1), the designed Ag diamond nanoantenna shows a better performance and a higher sensitivity.

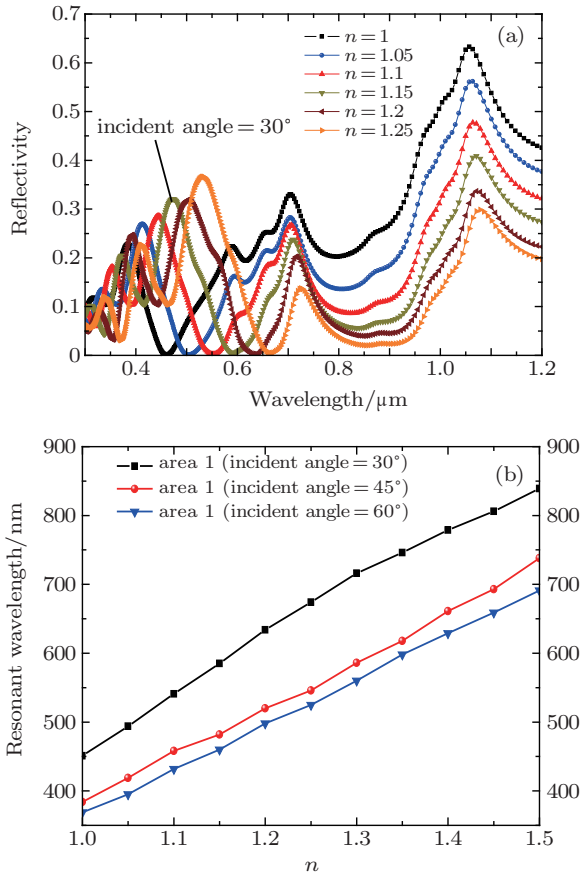


Fig. 6. (color online) (a) Reflection spectrum as a function of index n at an incident angle of 30°. (b) Relationship between resonant wavelength and index with different incident angles.

Table 1. Optimal parameters of Ag nanoparticles and the corresponding maximum enhancement factor.

Nanostructure	Sensitivity	Ref.
gold nanospheres	154–914 nm/RIU	[22]
gold nano rods	650 nm/RIU	[23]
hollow gold nano shell	408 nm/RIU	[24]
arrays of gold nanodisk	327 nm/RIU	[19]
gold nanorings	880 nm/RIU	[25]
nanocrescents	879 nm/RIU	[26]
gold/silver nanoalloys	131–625 nm/RIU	[27]
nanocross	710 nm/RIU	[28]
nanostars	218 nm/RIU	[29]

In addition, Ag diamond nanoantennas could also effectively distinguish chemical solutions based on their unique refractive indices. To prove this statement, we choose eight types of chemical solutions, including acetone, ethyl acetate, acetic anhydride, n-heptane, n-butyl alcohol, propylene glycol, ethylene glycol, and ethanol with refractive indices (at 20 °C) obtained from Ref. [30]. The reflection spectra corresponding to these eight chemical reagents are shown in Fig. 7.

As we can see, when the incident angle is 15°, the resonance amplitude becomes negligible in area 2. While in areas 1 and 3, strong resonance effect can still be observed. In area 1, different solutions are featured by different resonance wavelengths, which allows the determination of the type of solutions using resonance wavelength. As for area 3, reflectivity is more sensitive to the refractive index change, which enables the determination of solution type using reflectivity. The detection results are summarized in Fig. 8.

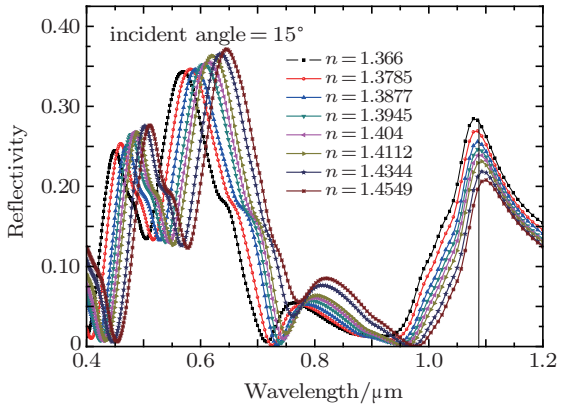


Fig. 7. (color online) Reflection spectrum corresponding to eight types of chemical reagents.

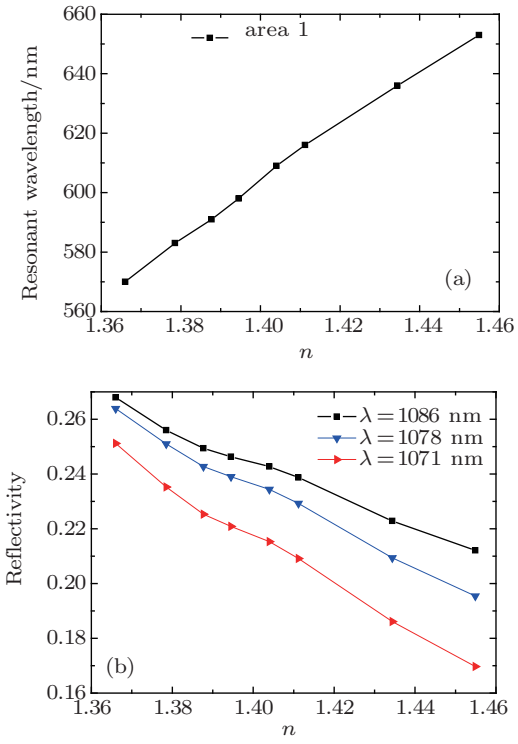


Fig. 8. (color online) (a) Resonant wavelength for eight kinds of chemical reagents in area 1. (b) Intensity reflectivity for eight kinds of chemical reagents at fixed wavelength in area 3.

In Fig. 8(a), the resonance wavelength still increases linearly with the refractive index with a detection sensitivity approaching 799 nm/RIU. Curves in Fig. 8(b) show that, for area 3, the reflectivities corresponding to three resonance wavelengths (1071, 1078, and 1086 nm) decrease linearly with the refractive index. The detection sensitivities are 0.91, 0.76, and 0.62 when the wavelengths are 1071, 1078, and 1086 nm, respectively.

To further investigate the sensing properties of Ag diamond nanoantennas, we choose different concentrations of

sucrose solutions and different ratios of ethanol and ethylene glycol solutions as experimental subjects. The sucrose solution has a linear relation between its concentration and index with a slope of 0.01 RIU per 5% concentration (0.01 RIU/5%). The refractive index of the mixed ethanol and ethylene glycol is equal to the composition of the refractive index ratio linear superposition, i.e., $R_{\text{mixed}} = R_1 \times \delta_1\% + R_2 \times \delta_2\%$, where δ_i stands for the proportion of substance 1 or 2.[31] The relations between the concentration (ratio) and index for these solutions (at 20 °C) are obtained from Ref. [30]. Experimental results for these solutions are presented in Fig. 9.

In Fig. 9, the resonant wavelength and reflectivity at fixed wavelengths for all solutions change linearly with the index. The detection sensitivities in Figs. 9(a) and 9(b) are 760 nm/RIU and 0.73 AU/RIU, respectively. The detection sensitivities in Figs. 9(c) and 9(d) are 981 nm/RIU and 0.93 AU/RIU, respectively. Therefore, we could conclude that Ag diamond nanoantennas can be used to detect the environmental index by measuring the resonant wavelength and reflectivity at fixed wavelengths with high sensitivity.

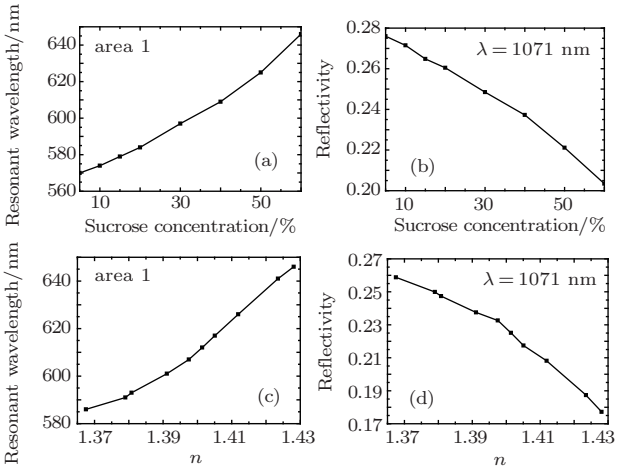


Fig. 9. (a) Resonant wavelength and concentration for sucrose in area 1. (b) Intensity reflectivity and concentration for sucrose in area 3. (c) Relationship between resonance wavelength and index for ratios of solution. (d) Relationship between reflectivity and index for ratios of solution.

4. Conclusion

In this paper, we investigate the light trapping properties of Ag diamond nanoantennas as well as its capability in detecting the refraction indices, solultion concentrations, and solution allocation ratios using numerical analysis. The absorption enhancement of thin-film solar cells with diamond nanoantennas is also numerically investigated. The presence of Ag nanoantennas has been demonstrated to greatly enhance light absorption over a broad range of wavelengths, especially in the near infrared region due to the LSPR effect. The maximum enhancement factor $G = 1.51$ can be obtained when $h = 60$ nm, $P_x = 30$ nm, $P_y = 90$ nm, $a = 20$ nm, and $b = 85$ nm. In addition, Ag diamond nanoantennas could help to greatly improve the detection sensitivity and the sensitivity of the resonant spectrum dependence on the environmental indices is studied. Optimal incident angle of 15° could achieve a maximum detection sensitivity of about 837 nm/RIU and a resolution of about 10^{-3} RIU when the resonant wavelength is used to detect the environmental indices. Moreover, we achieve a sensitivity of about 0.93 AU/RIU when using reflectivity at fixed wavelength. Finally, the detection of three properties of solutions is analyzed, suggesting that the designed nanoantennas are quite effective in solution detection. In conclusion, Ag diamond nanoantennas can detect the environmental index with high sensitivity, which would be useful in biosensor and biotechnology.

References

[1] Wollschläger J, Nicolaus A, Wiltshire K H and Metfies K 2014 *J. Plankton Res.* **36** 695
[2] Zhang Z Y, Wang L N, Hu H F, Li K W, Ma X P and Song G F 2013 *Chin. Phys. B* **22** 014213
[3] Hajizadegan M, Ahmadi V and Sakhdari M 2013 *J. Lightw. Tech.* **31** 1877
[4] Chen F, Cheng J, Dai S, Xu Y and Yu Q 2013 *Mater. Res. Bull.* **48** 4667
[5] Wu P, Xu W, Li L L, Lu T C and Wu W D 2014 *Chin. Phys. B* **23** 107807
[6] Tok R U and Şendur K 2013 *Opt. Lett.* **38** 3119
[7] Catchpole K R and Polman A 2008 *Opt. Express* **16** 21793
[8] Chopra1 K L, Paulson P D and Dutta V 2004 *Progress in Photovoltaics: Research and Applications* **12** 69
[9] Li Z Y, Liu J and Zhong X L 2014 *Chin. Phys. B* **23** 047306
[10] Prasad M R, Deena S, Rajesh C, Pandit V K and Pathan H M 2013 *J. Renew. Sustain. Ener.* **5** 031615
[11] Cao J, Tong S and Grattan K T V 2014 *Sensor. Actuat. B* **195** 332
[12] Liu F, Wong M M K, Chiu S K, Lin H, Ho J C and Pang S W 2014 *Biosens. Bioelectron.* **55** 141
[13] Wei A, Zhu T and Zhu Q Z 2014 *J. Quant. Spectro. Rad. Trans.* **132** 28
[14] Manera M G and Rella R 2013 *Sensor. Actuat. B* **179** 175
[15] Feng D J, Liu G X, Zhang M S and Jia D F 2013 *Chin. Opt. Lett.* **11** 110607
[16] Hamidi Z S, Chumiran S H, Mohamad A, Shariff N N M, Ibrahim Z A, Radzin N, Hamzan N, Anim N M and Alias A N 2013 *Am. J. Mod. Phys.* **2** 58
[17] Neumann L, Van't Oever J and Van Hulst N F 2013 *Nano Lett.* **13** 5070
[18] Jalilvand M, Li X, Kowalewski J and Zwick T 2014 *Electron. Lett.* **50** 244
[19] Cetin A E, Yanik A A, Yilmaz C, Somu S, Busnaina A and Altug H 2011 *Appl. Phys. Lett.* **98** 111110
[20] Palik E D 1985 *Handbook of Optical Constants of Solids* (San Diego: Academic Press) p. 555
[21] http://rredc.nrel.gov/solar/spectra/am1.5/ASTMG173/ASTMG173.html
[22] Tu M H, Sun T and Grattan K T V 2012 *Sensor. Actuat. B* **164** 43
[23] Lee K S and Mostafa A 2006 *J. Phys. Chem. B* **110** 19220
[24] Sun Y G and Xia Y N 2002 *Anal. Chem.* **74** 5297
[25] Larsson E M, Alegret J, Käll M and Sutherland D S 2007 *Nano Lett.* **7** 1256
[26] Bukasov R, Ali T A, Nordlander P and Shumaker-Parry J S 2010 *ACS Nano* **4** 6639
[27] Tu H E, Tong S and Kenneth T G 2013 *Sensor. J. IEEE* **132013** 2192
[28] Verellen N, Van Dorpe P, Huang C, Lodewijks K, Vandenbosch G A, Lagae L and Moshchalkov V V 2011 *Nano Lett.* **11** 391
[29] Dondapati S K, Sau T K, Hrelescu C, Klar T A, Stefani F D and Feldmann J 2010 *ACS Nano* **4** 6318
[30] *Refractive Index Concentration Tables* (Extreme Networks, 2012)
[31] Ye D N 1965 *Chin. Sci. Bull.* **9** 816